CONTROL OF THE POWER GENERATED BY VARIABLE SPEED WIND TURBINE DRIVING A DOUBLY FED INDUCTION GENERATOR

R. ROUABHI[1] ,Ali DJERIOUI[2]
(1) Department of Electrical Engineering, Batna University,Algeria, tel: 0662580979 (2) Department of Electrical Engineering, USTHB University, Algeria.
. Email: riyadhrouabhi@gmail.com. alidjerioui@yahoo.fr

Abstract: *This paper is interested in the study of a wind energy conversion system (WECS) based on a doubly fed induction generator (DFIG) connected to the electric power grid. The objective of our work is to make a modeling of a various components of the wind system, therefore using these models to work out a control device which allows the improvement of the production's quality of electrical energy. For that purpose, I'm going to present to you a strategy of control by vector control (PI Classical) to control independently the active and reactive powers generated by the DFIG uncoupled by flux orientation*

Key words: *Wind turbine, Modeling, DFIM, MPPT, Vector control, Bidirectional converter.*

1. Introduction

Over the last twenty years, renewable energy sources have been attracting great attention due to the cost increase, limited reserves, and adverse environmental impact of fossil fuels. In the meantime, technological advancements, cost reduction, and governmental incentives have made some renewable energy sources more competitive in the market. Among them, wind energy is one of the fastest growing renewable energy sources [1].

Installed wind power capacity has been progressively growing over the last two decades. The installed capacity of global wind power has increased exponentially from approximately 6 GW in 1996 to 158 GW by 2009. The wind industry has achieved an average growth rate of over 25% since 2000, and is expected to continue this trend in the coming years. This impressive growth has been spurred by the continuous cost increase of classic energy sources, cost reduction of wind turbines, governmental incentive programs, and public demand for cleaner energy sources. Although Europe has maintained its role as the largest wind power producer as a region, the Unites States has surpassed the long-time world leader Germany by increasing its installed capacity of almost 50% in just two years. It has now an installed capacity of 35 GW, equivalent to 22.3% of the global installed capacity. Asian countries are catching up, mainly driven by the markets in China and India. In fact, China doubled its installed capacity in one year, and is expected to continue to grow at a fast pace in the next few years [2].Our study aims primarily the conversion of wind energy into electrical energy by the use of a DFIG controlled through the rotor sizes, and supplied with a cascade based on two converters PWM on two levels. The principal function of these converters in the conversion system of wind energy is the connection of wind generator to the electrical communication with a double vision: to control independently of the active and reactive powers generated by the DFIG. With this intention, several strategies of control are proposed in the literature in order to control these converters.

2. Modeling of the wind system

For facilitating the study and the control of the chain of conversion, we will describe a model for each component of our system.

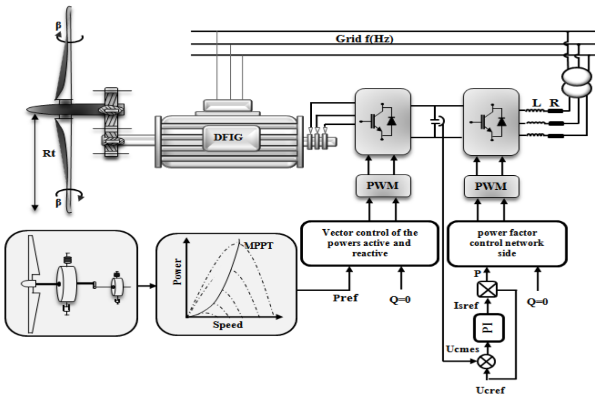

Fig. 1. Synoptic diagram of the WECS.

2.1 Modeling and control of the turbine

Modeling of the turbine

The aerodynamic (mechanical) power that the wind turbine extracts from the wind is expressed by the following equation:

$$P_m = \frac{1}{2}.\rho.\pi.R_T^2.V^3.C_p(\lambda, \beta) \qquad (1)$$

Where ρ is the air density, R_T is the wind turbine rotor radius, V is the wind speed, and the power coefficient $Cp\ (\lambda,\ \beta)$ represents the turbine efficiency to convert the kinetic energy of the wind into mechanical energy [3]. This coefficient is a function of both the blade pitch angle β and the tip speed ratio λ, which is defined as [4]:

$$\lambda = \frac{\Omega_T . R_T}{V} \tag{2}$$

Where Ω_T is the shaft speed (in rad/sec). As a matter of example, the expression of the power coefficient of a wind turbine of *4*Kw is approximated by the equation:

$$C_p(\lambda,\beta) = \left(0,5 - 0,0167.(\beta-2)\right).\sin\left[\frac{\pi.(\lambda+0,1)}{18,5-0,3.(\beta-2)}\right] - 0,00184.(\lambda-3).(\beta-2) \tag{3}$$

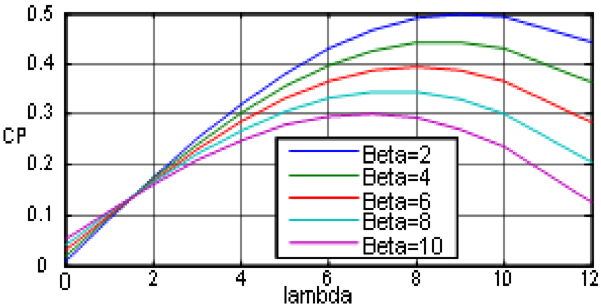

Fig. 2. Power coefficient Cp according to λ for different β.

$$C_g = \frac{C_T}{G} \quad , \quad \Omega_T = \frac{\Omega_g}{G} \quad ,$$

$$\frac{C_T}{G} - C_g = J.\frac{d\Omega_g}{dt} + f.\Omega_g \tag{4}$$

Thus, we can establish the model of the turbine whose diagram block is given on the figure below.

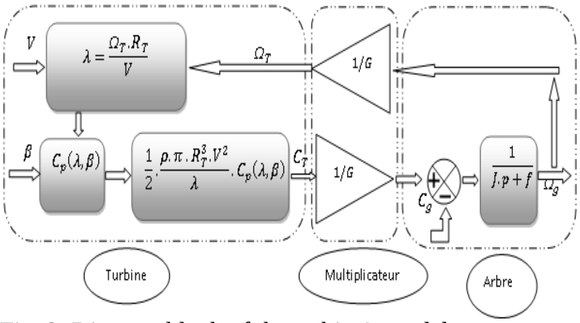

Fig. 3. Diagram block of the turbine's model.

Control in lower part of the nominal output (optimization of the power)

In this zone of the operation, the control has as main objectives are to maximize the captured energy of the wind and to minimize the efforts undergone by the driving mechanism. To maximize the capture of the energy of the wind, there are two variables must be maintained with their optimal values in control to ensure the maximum value of *Cp(opt) = (λopt ,βopt)* [5].

One by fixing the pitch angle at it optimal value *βopt ,* and the other by fixing the specific speed to its optimal value *λopt* . The characteristic corresponding to this relation is given in Zone II of the figure 4.

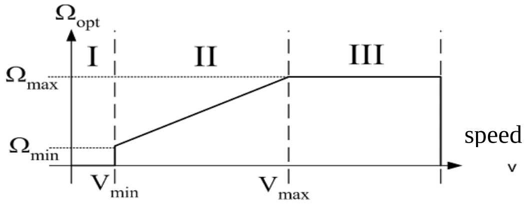

Fig. 4. Ideal characteristic of a wind turbine at variable speed

Zone I: corresponds with the very low speeds of the insufficient wind to actuate the wind system.
Zone III: corresponds with the very high speeds of the wind, the objective in this zone is to limit the output power to a value equal to the nominal power of the wind system to avoid overloads. This is done by action on the pitch angle of the blades.

➢ *INDIRECT CONTROL IN ZONE II.*

The technique of optimization of the power used in this zone is the MPPT control. In this paper, the WT operates with a constant pitch angle *β=2* deg and from Fig. 2. The maximum power coefficient *Cp max=0.5* is achieved for a tip speed ratio value *λ=9.2*.

$$C_{Topt} = \frac{1}{2}.\rho.\pi.R_T^3.V^2 \frac{C_p(\lambda_{opt})}{\lambda_{opt}} \tag{5}$$

$$V = \frac{R_T . \Omega_T}{\lambda_{opt}} \tag{6}$$

$$C_{Topt} = \frac{1}{2}.\rho.\pi.R_T^5.\frac{C_p(\lambda_{opt})}{\lambda_{opt}^3}.\Omega_T^3 \tag{7}$$

$$C_{Topt} = k_{opt}.\Omega_T^2 \quad \text{and} \quad k_{opt} = \frac{1}{2}.\rho.\pi.R_T^5.\frac{C_p(\lambda_{opt})}{\lambda_{opt}^3},$$

$$\frac{C_T}{G} - C_g - f.\Omega_g = 0 \quad \text{and} \quad \frac{k_{opt}}{G}.\Omega_T^2 - f.\Omega_g - C_g = 0 \quad \textit{with:}$$

$$\Omega_g = G.\Omega_T \quad \text{then} \quad C_{gopt} = \frac{k_{opt}}{G^3}.\Omega_g^2 - f.\Omega_g$$

The control's diagram block structure is given by the figure below.

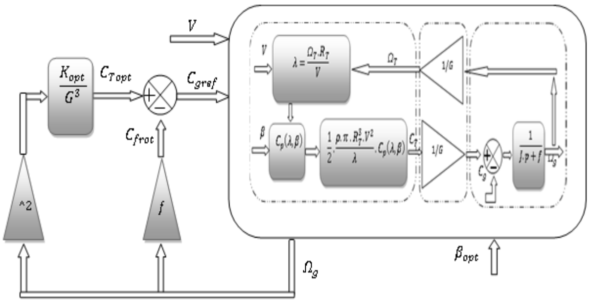

Fig. 5. Indirect control speed (Zone II).

2.2 Modeling of the Generator

The mathematical model of a doubly fed induction generator in the rotating frame (*d-q*) can be described by the following equations [6,7,8,9]:

$$\begin{cases} V_{sd} = R_s I_{sd} + \dfrac{d\varphi_{sd}}{dt} - w_s \varphi_{sq} \\ V_{sq} = R_s I_{sq} + \dfrac{d\varphi_{sq}}{dt} + w_s \varphi_{sd} \\ V_{rd} = R_r I_{rd} + \dfrac{d\varphi_{rd}}{dt} - w_r \varphi_{rq} \\ V_{rq} = R_r I_{rq} + \dfrac{d\varphi_{rq}}{dt} + w_r \varphi_{rd} \end{cases} \& \begin{cases} \varphi_{sd} = L_s I_{sd} + M I_{rd} \\ \varphi_{sq} = L_s I_{sq} + M I_{rq} \\ \varphi_{rd} = L_r I_{rd} + M I_{sd} \\ \varphi_{rq} = L_r I_{rq} + M I_{sq} \end{cases} \quad (8)$$

The electromagnetic torque equation is given by:

$$C_{em} = p\,\frac{M}{L_s}\left(I_{rd}\,\varphi_{sq} - I_{rq}\,\varphi_{sd}\right) \quad (9)$$

The stator active and reactive powers are expressed by:

$$\begin{cases} P = V_{sd} I_{sd} + V_{sq} I_{sq} \\ Q = V_{sq} I_{sd} - V_{sd} I_{sq} \end{cases} \quad (10)$$

Setting in the form of equation of state

Our goal is to represent the equations established above in the following form:

$$\left[\dot{X}\right] = [A].[X] + [B].[U] \quad (11)$$

With:

$$[X] = \left[\varphi_{sd} \quad \varphi_{sq} \quad i_{rd} \quad i_{rq}\right]^t; \qquad [U] = \left[v_{sd} \quad v_{sq} \quad v_{rd} \quad v_{rq}\right]^t;$$

$$[A] = \begin{bmatrix} \dfrac{-1}{T_s} & w_s & \dfrac{M}{T_s} & 0 \\ -w_s & \dfrac{-1}{T_s} & 0 & \dfrac{M}{T_s} \\ \alpha & -\beta w_e & -\delta & w_r \\ \beta w_e & \alpha & -w_r & -\delta \end{bmatrix}, [B] = \begin{bmatrix} 1 & 0 & 0 & 0 \\ 0 & 1 & 0 & 0 \\ \dfrac{-M}{\sigma L_r L_s} & 0 & \dfrac{1}{\sigma L_r} & 0 \\ 0 & \dfrac{-M}{\sigma L_r L_s} & 0 & \dfrac{1}{\sigma L_r} \end{bmatrix};$$

α , β and δ are constants define as follows:

$$\alpha = \frac{M}{\sigma T_s L_s L_r}; \qquad \beta = \frac{M}{\sigma L_s L_r};$$

$$\delta = \frac{1}{\sigma}\left(\frac{1}{T_r} + \frac{M^2}{T_s L_r L_s}\right); \quad w_e = w_s - w_r$$

2.3 Modeling and control of the grid side converter

The Rotor side converter is used to providing bi-directed flowed channel for rotor-side converter, stabilizing the DC-link voltage and achieving unity power factor or changed power factor of grid-side [10].

Modeling of the grid side converter

The source of feed:

$$\frac{d}{dt}\begin{bmatrix} i_1 \\ i_2 \\ i_3 \end{bmatrix} = \begin{bmatrix} -\dfrac{R}{L} & 0 & 0 \\ 0 & -\dfrac{R}{L} & 0 \\ 0 & 0 & -\dfrac{R}{L} \end{bmatrix} \begin{bmatrix} i_1 \\ i_2 \\ i_3 \end{bmatrix} + \frac{1}{L}\begin{bmatrix} V_1 - V_{an} \\ V_2 - V_{bn} \\ V_3 - V_{cn} \end{bmatrix} \quad (12)$$

The Converter:

$$\begin{bmatrix} V_A \\ V_B \\ V_C \end{bmatrix} = \frac{Uc}{3}.\begin{bmatrix} 2 & -1 & -1 \\ -1 & 2 & -1 \\ -1 & -1 & 2 \end{bmatrix}\begin{bmatrix} S_1 \\ S_2 \\ S_3 \end{bmatrix} \quad (13)$$

In more, the rectified current is given by:

$$i_s = \left[S_1 \ S_2 \ S_3\right]\begin{bmatrix} i_1 \\ i_2 \\ i_3 \end{bmatrix} \quad (14)$$

$$\begin{cases} \dfrac{dU_C}{dt} = \dfrac{1}{C}\left(i_s - i_L\right) \\ U_C = R_{Ch}.i_L \end{cases} , \qquad \frac{U_C}{i_s} = \frac{R_{Ch}}{1 + R_{Ch}.C.p} \quad (15)$$

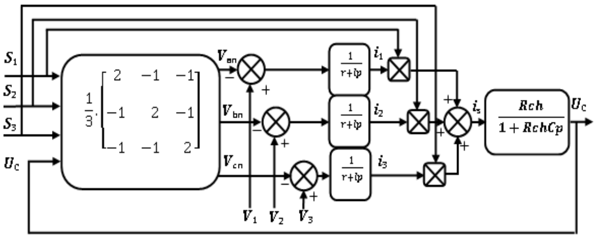

Fig. 6. Functional diagram of the grid side converter.

Grid side converter control

The objective of the grid side converter is to regulate the DC-link voltage and to set a unit power factor. A vector control approach is used with a reference frame oriented along the grid voltage vector, enabling independent control of the DC link voltage and the reactive power flowing between the grid and the grid side converter. Figure 6 illustrates the whole bloc diagram of the grid side converter control [11].

➢ Modeling in the frame mark (*d,q*)

Equations that governing the system are:

$$\begin{cases} V_{pd} = V_d - R.i_d - L\dfrac{di_d}{dt} + Lw.I_q \\ V_{pq} = V_q - R.i_q - L\dfrac{di_q}{dt} + Lw.I_d \end{cases} \qquad (16)$$

V_{pd} and V_{pq} : are the components of Park of the converter's input voltages. V_d and V_q : Park's Components of the grid voltages. i_d and i_q : Park's Components of the grid currents. w : Pulsation of the grid.

The expressions of the active and reactive powers are given by:

$$\begin{cases} P = \dfrac{3}{2}\left[V_d I_d + V_q I_q\right] \\ Q = \dfrac{3}{2}\left[V_q I_d + V_d I_q\right] \end{cases} \qquad (17)$$

This system can be written in the following metric form:

$$\begin{bmatrix} P \\ Q \end{bmatrix} = \frac{3}{2}.\begin{bmatrix} V_d & V_q \\ V_q & -V_d \end{bmatrix}\begin{bmatrix} i_d \\ i_q \end{bmatrix} \qquad (18)$$

And we set $P = U_c I_s$ *and* $Q = 0$

The diagram block of the regulation is then represented in the figure below.

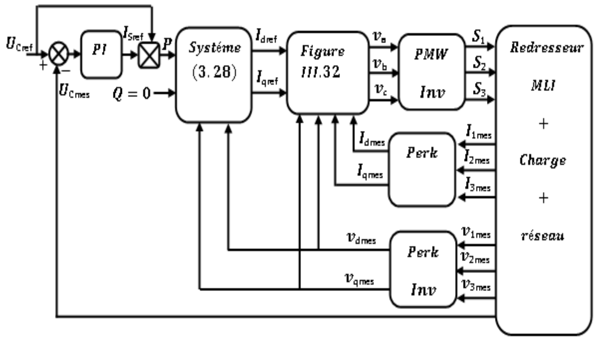

Fig.7. The control while running of the rectifier with PWM in the reference mark (d,q).

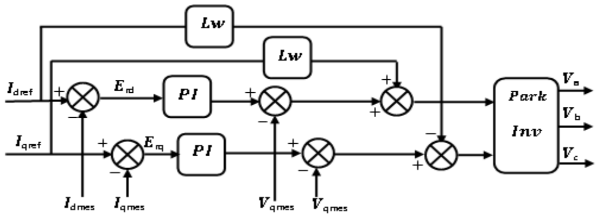

Fig.8. bloc diagram of the GSC current control in Park reference frame.

Simulation and interpretation of the results

It is clear that the direct voltage follows the imposed reference Figure 9. In more, the currents of line follow their references perfectly and have a sinusoidal form Figure 10. What confirms the advantage of the PWM rectifier in the reduction of the harmonics.

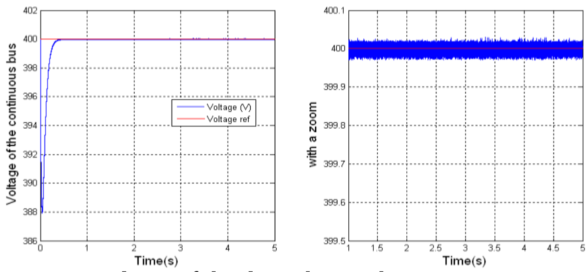

Fig. 9. Voltage of the direct bus with a zoom.

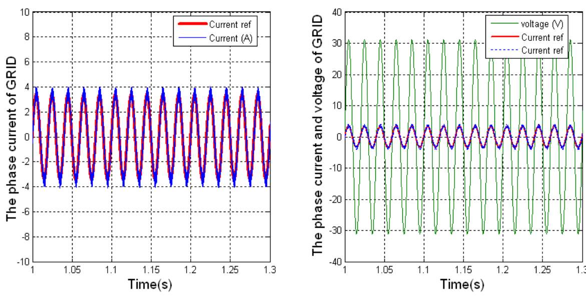

Fig. 10. Current and tension of line.

2.4 Modeling of the inverter

The Rotor side converter is used to control the active and reactive powers injected by the stator of the doubly fed induction generator to the grid. The inverter used is a simple three-phase inverter on two levels (six switches) [12].

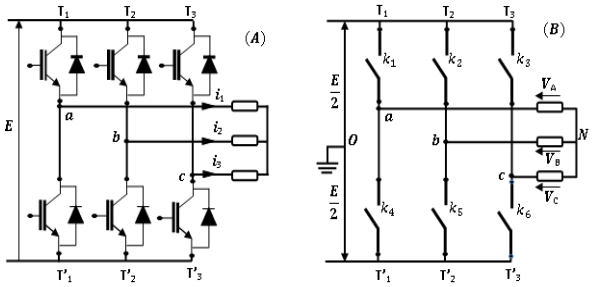

Fig. 11. the three- phases inverter on two levels.

The mathematical model of the three-phases inverter.

$$\begin{bmatrix} V_A \\ V_B \\ V_C \end{bmatrix} = \frac{E}{6} \cdot \begin{bmatrix} 2 & -1 & -1 \\ -1 & 2 & -1 \\ -1 & -1 & 2 \end{bmatrix} \begin{bmatrix} S_1 \\ S_2 \\ S_3 \end{bmatrix} \tag{19}$$

3. Vector control of the powers active and reactive

The vector control orientation of the flow has an attractive solution to achieve better performance in variable speed applications in the case of the DFIM as well under operation generator as motor [13].

In this context, we proposed a control law for DFIM based on the orientation of the stator flux, used to run a generator. The latter highlights the relationship between the stator and rotor Ingredients. These relationships will help to act on the rotor signals to control the exchange of active and reactive power between the stator of the machine and the grid. With a constant and directed stator flux, $\varphi_{sd} = \varphi_s$ et $\varphi_{sq} = 0$ [14], if we neglects the resistance of the stator windings, the equations of the tensions of the machine are reduced to the following form [15, 16]:

$$\begin{cases} V_{sd} = 0 \\ V_{sq} = V_s = w_s.\varphi_s \\ V_{rd} = R_r.I_{rd} + \dfrac{d\varphi_{rd}}{dt} - w_r\varphi_{rq} \\ V_{rq} = R_r.I_{rq} + \dfrac{d\varphi_{rq}}{dt} + w_r\varphi_{rd} \end{cases} \tag{20}$$

The equations of flux are expressed by:

$$\begin{cases} \varphi_{sd} = \varphi_s = L_s.I_{sd} + M.I_{rd} \\ 0 = L_s.I_{sq} + M.\varphi_{rq}. \\ \varphi_{rd} = L_r.I_{rd} + M.\varphi_{sd}. \\ \varphi_{rq} = L_r.I_{rq} + M.\varphi_{sq}. \end{cases} \tag{21}$$

The stator active and reactive powers are expressed by:

$$\begin{cases} P_s = -\dfrac{V_s.M}{L_s}.I_{rq} \\ Q_s = \dfrac{V_s^2}{w_s.L_s} - \dfrac{V_s.M}{L_s}.I_{rd} \end{cases} \tag{22}$$

The Stator components of the current are expressed by:

$$\begin{cases} I_{rq} = -\dfrac{L_s}{V_s.M}.P_s \\ I_{rd} = \dfrac{V_s^2}{w_s.L_s} - \dfrac{L_s}{V_s.M}.Q_s \end{cases} \tag{23}$$

Components out of phase of the rotor tensions:

$$\begin{cases} V_{rd} = \left[R_r + \left(L_r - \dfrac{M^2}{L_s}\right)s\right] I_{rd} - g.w_s\left(L_r - \dfrac{M^2}{L_s}\right).I_{rq} \\ V_{rq} = \left[R_r + \left(L_r - \dfrac{M^2}{L_s}\right)s\right] I_{rq} + g.w_s\left(L_r - \dfrac{M^2}{L_s}\right).I_{rd} + g.\dfrac{V_s.M}{L_s} \end{cases} \tag{24}$$

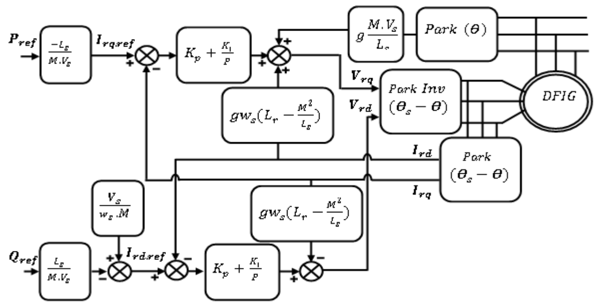

Fig.12. Diagram block of the structure of control by orientation of the stator flux of the DFIG fed in tension

3.1 Simulation and interpretation of the results

Results without turbine (speed fixes)

The results of simulation present the various curves obtained by the vector control in active and reactive powers generated on the level of the stator of the DFIG. A good follow-up of instruction for the active and reactive powers stator is noted.

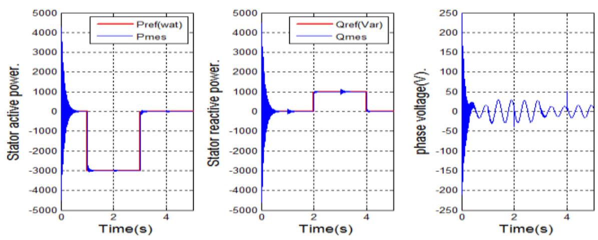

Fig. 13. The active and reactive powers and the rotor voltage.

Results with turbine (variable speed)

The figures below show the performances of the cascade using a rectifier and an inverter on two levels connects to the rotor of the DFIG which is pulled by a wind turbine. The control of the rectifier consists with two control loops.

The setpoint of the stator active power is given starting from the power of the turbine. We notes a good follow-up of setpoint for the active power as well as the stator reactive power which is maintained null by the real powers output by the DFIG. This technique made it possible to obtain a perfect decoupling between the two components of the stator power.

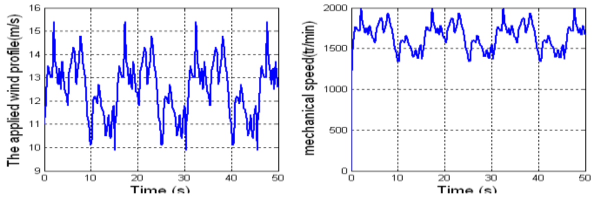

Fig.14. The applied wind profile and mechanical speed.

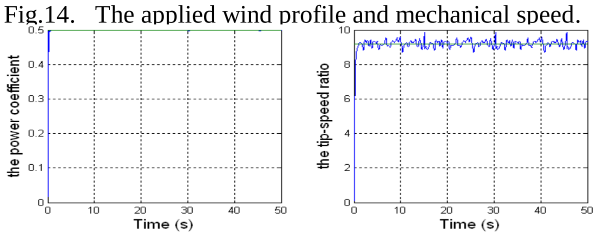

Fig.15. The tip-speed ratio and the power coefficient

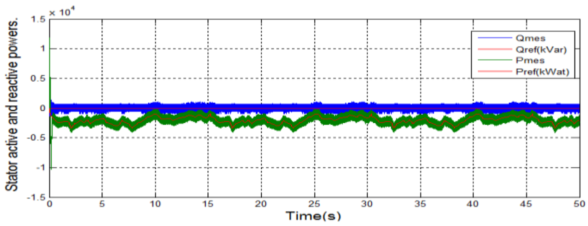

Fig.16. The stator active and reactive powers.

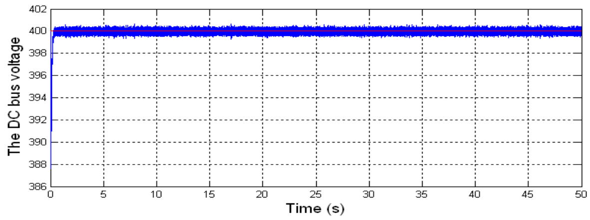

Fig.17. The DC bus voltage.

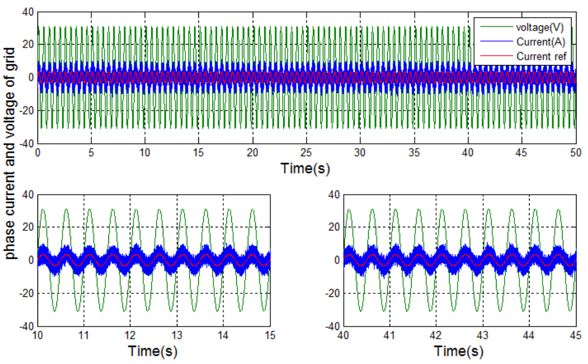

Fig.19. The phase current and voltage of grid.

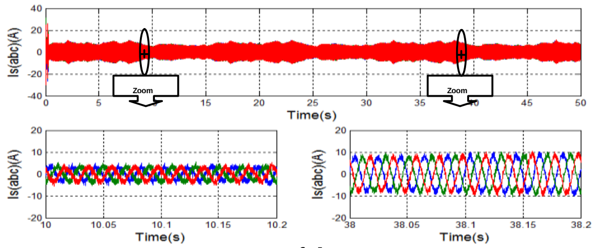

Fig.18. Stator components of the current.

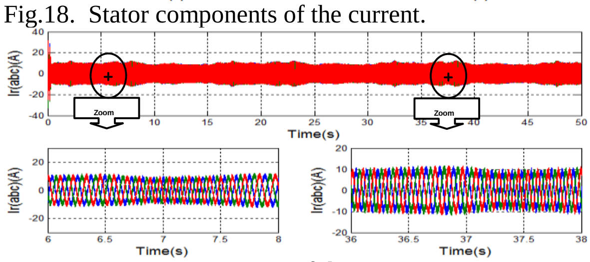

Fig.19. Rotor components of the current.

4. Conclusion

This work enabled us to study and apply the vector control for the regulation of stator's active and reactive powers in system of production of wind energy. The vector control that using DFIG of traditional regulators PI presents certain disadvantages such as the sensitivity to parametric uncertainties of the machine and their variations.

References

1. M. E.El-Hawary *(Principles of Electric Machines with Power Electronic Applications).* Second Edition

2. By B. Wu, Y. Lang, N. Zargari, and S. Kouro *(Power conversion and control of wind energy systems).* © 2011 the Institute of Electrical and Electronics Engineers, Inc. Published (2011) by John Wiley & Sons.

3. F. D. Bianchi, R. J. Mantz, and C. F. Christiansen, *(Gain scheduling control of variable-speed wind energy conversion systems using quasilpv models)* Control Engineering Practice, vol. 13, no. 2, pp. 247 –255, 2005.

4. W. Qiao, L. Qu, and R. Harley, *(Control of IPM synchronous generator for maximum wind power generation considering magnetic saturation)* IEEE Transactions on Industry Applications, vol. 45, no. 3, pp. 1095–1105, may-june 2009.

5. Y Xia, K.H Ahmed, B.W. Williams,*(A New Maximum Power Point Tracking Technique for Permanent Magnet Synchronous Generator Based Wind Energy Conversion System,)* IEEE Transactions on Power Electronics, Vol. 26, No. 12, pp. 3609 – 3620, December 2011.

6. V. CALDERARO, V. GALDI, A. PICCOLO, P. SIANO. *(A fuzzy controller for maximum energy extraction from variable speed wind power generation systems).* Electric Power Systems Research, Volume 78, Issue 6, pp 1109-1118, Elsevier (2008).

7. Yongchang Zhang, Jianguo Zhu, Jiefeng Hu *(Model*

predictive Direct torque control for grid Synchronization of Doubly Fed Induction Generator). Proceedings of the 2011 IEEE. International Electric Machines & Drives Conference (IEMDC) 15-18 May 2011 Niagara Falls, , pp. 765 –770.

8. Victor Flores Mendes, Clodualdo Venicio de Sousa, Selˆenio Rocha Silva, Balduino Cezar Rabelo, Jr., and Wilfried Hofmann, Senior Member, IEEE. *(Modeling and Ride-Through Control of Doubly Fed Induction Generators During Symmetrical Voltage Sags)*.IEEE Trans. Energy Convers., VOL. 26, NO.4, pp. 1161–1171, DEC 2011.

9. Esmaeil Rezaei, Ahmadreza Tabesh, Member, IEEE, and Mohammad Ebrahimi. *(Dynamic Model and Control of DFIG Wind Energy Systems Based on Power Transfer Matrix)*.IEEE Trans. Energy Convers., VOL. 27, NO. 3, pp. 1485–1493, JULY 2012.

10. Haisheng Sun, Yongfeng Ren , Hanshan LiZhongquan An, Jinguo Liu, Hongbin Hu and Haitao Liu(*DFIG Wind Power Generation Based on Back-to-back PWM Converter)*. Proceedings of the 2009 IEEE. International Conference on Mechatronics and Automation.August 9 -12, Changchun, China, pp. 2276 –2280.

11. T. Ghennam, E.M. Berkouk, B. François (*Modeling and Control of a Doubly Fed Induction Generator (DFIG) Based Wind Conversion System*), POWERENG, Lisbon, Portugal, March 18-20, IEEE 09. pp. 507 –512.

12. Vincenzo Galdi, Member, IEEE, Antonio Piccolo, and Pierluigi *Siano (Designing an Adaptive Fuzzy Controller for Maximum Wind Energy Extraction*) .IEEE transactions on energy conversion, vol. 23, no. 2, pp. 559 –569, june 2008.

13. P.C. Krause, O. Wasynczuk, S.D. Sudhoff, *(Analysis of Electric Machinery)*, IEEE Press, Piscataway, NJ, 1995.
14. D. AOUZELLAG, E.M. BERKOUK, *(Network power flux control of a wind generator).* Renewable Energy, Volume 34, Issue 3, pp 615- 622, Elsevier (2009).

15. I.Boldea *(Variable speed gener)* Taylor & Francis2006.

16. K. GHEDAMSIA, E.M. BERKOUK. *(Control of wind generator associated to a flywheel energy storage system).* Renewable Energy, Volume 33, Issue 9, pp 2145-2156, Elsevier (2008).

17. A. DJERIOUI, K. ALIOUANE, F.BOUCHAFAA *(Direct power Control strategy for PWM Rectifier With the function of an Active Power Filter Based on a Novel Virtual Flux Observer).* journal electrical engineering, vol 13/2013 edition 1.
18. M. Liserre, R. Cárdenas, M. Molinas, J. Rodríguez, Overview of multi-MW wind turbines and wind parks, IEEE Transactions on Industrial Electronics 58 (2011) 1081–1095.
19. Ki-Hong Kim; Yoon-Cheul Jeung; Dong-Choon Lee; Heung-Geun Kim, "LVRT Scheme of PMSG Wind Power Systems Based on Feedback Linearization," Power Electronics, IEEE Transactions on , vol.27, no.5, pp.2376,2384, May 2012.